Antarctic Science

Supplemental Material for "**Winter climate change on the northern and southern Antarctic Peninsula**" by Evtushevsky O.M., Kravchenko V.O., Grytsai A.V., and Milinevsky G.P.

Corresponding authors: Oleksandr Evtushevsky, o_evtush@ukr.net; Gennadi Milinevsky, genmilinevsky@jlu.edu.cn; Taras Shevchenko National University of Kyiv, Kyiv, Ukraine.

Figure S1 shows that a half-century warming across the Antarctic Peninsula (upper panel) occurred in each seasons by 2–5°C. The recent cooling or absence of warming in the annual mean temperature (Fig. S1j) was mainly due to negative trends in spring and summer (Fig. S1g & S1h). The trend was slightly positive in autumn (Fig. S1i).

The winter warming tendency observed in the preceding period (Fig. S1a) continued only in the northern peninsula (Fig. S1f). In the southern peninsula, as well as in most of the Antarctic region, the cooling by 1˚C to 2˚C prevailed (blue in Fig. S1b). Note the contrast between seasonally persistent warming in 1951–2005 (Fig. S1a–S1d) and seasonal diversity of temperature change in 2006–2017 (Fig. S1f–S1i).

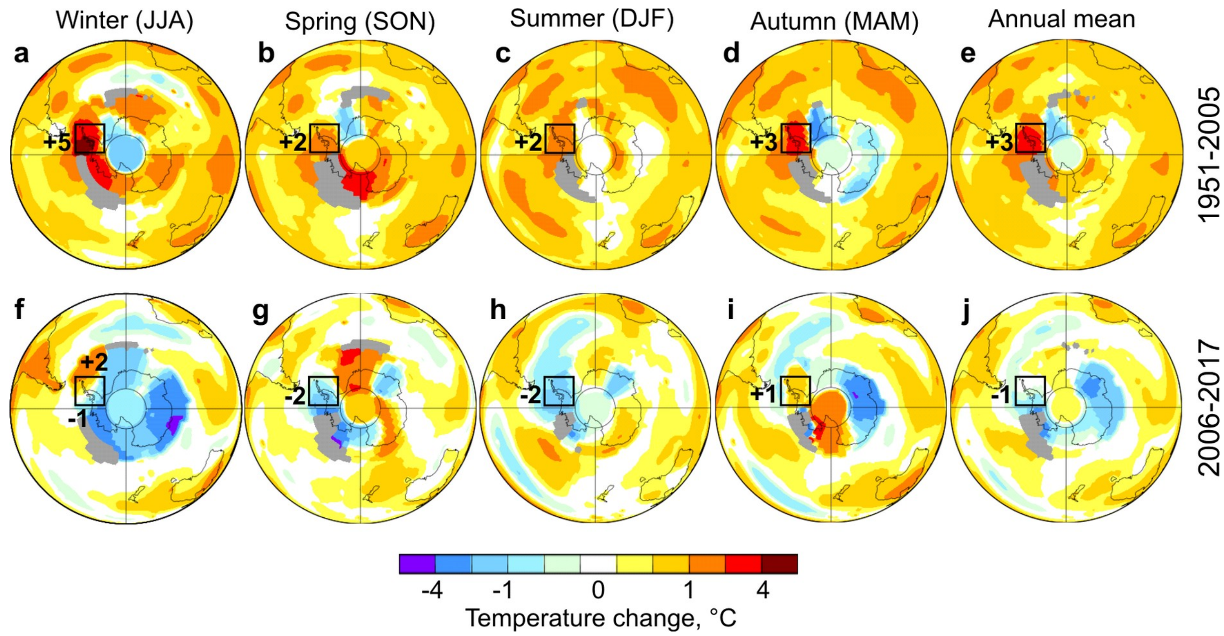

Fig. S1. Temperature changes in the Southern Hemisphere in (upper panel) 1951–2005 and (lower panel) 2006–2017 by **a.–d.** & **f.–i.** seasonal means and **e.** & **j.** annual means. The NASA GISS Surface Temperature Analysis data obtained from https://data.giss.nasa.gov/gistemp/maps. The Antarctic Peninsula region is bounded by a rectangle. Numbers show the total temperature changes (based on the color scale) in the corresponding period, season, or annual mean.

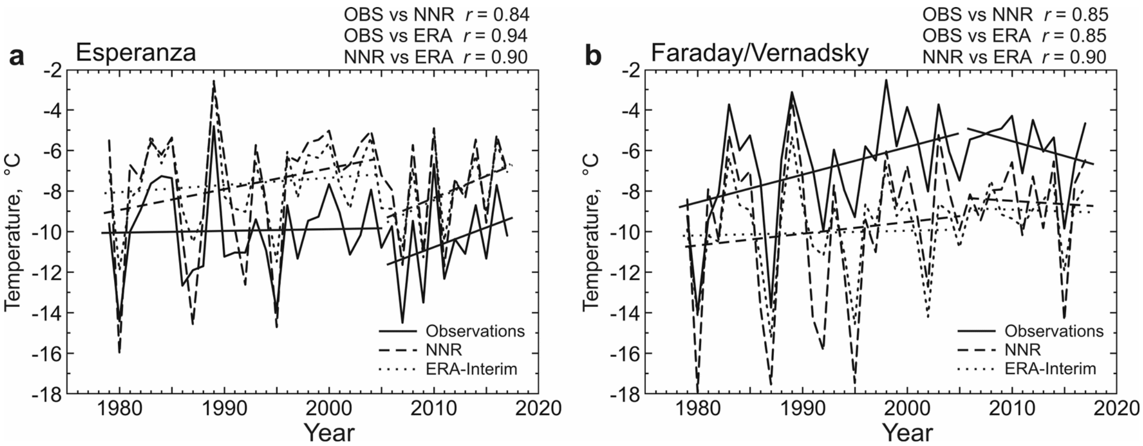

Fig. S2. Winter temperature time series for **a.** Esperanza and **b.** Faraday/Vernadsky. Observed temperature (solid lines), surface temperature from NCEP–NCAR reanalysis (dashed lines) and 2-m temperature from ERA-Interim (dotted lines) are presented. Piecewise linear trends for 1979–2005 and 2006–2017 are shown. Correlation coefficients between time series are indicated at the top.

The curves in Fig. S3a & S3b show wintertime (June–August) variability of the climate indices SAM from https://legacy.bas.ac.uk/met/gjma/sam.html and Niño-4 (N4) available at https://www.esrl.noaa.gov/psd/data/correlation/nina4.data, respectively, during the period 1950s–2010s.

Both curves demonstrate increasing trends in total time series and in separate periods indicated on the plots. As the couplings between the climate indices and the northern and southern peninsula are changing from statistically significant to insignificant on decadal time scale (Fig. 11), the SAM and N4 increasing trends do not always contribute to warming in different parts of the peninsula.

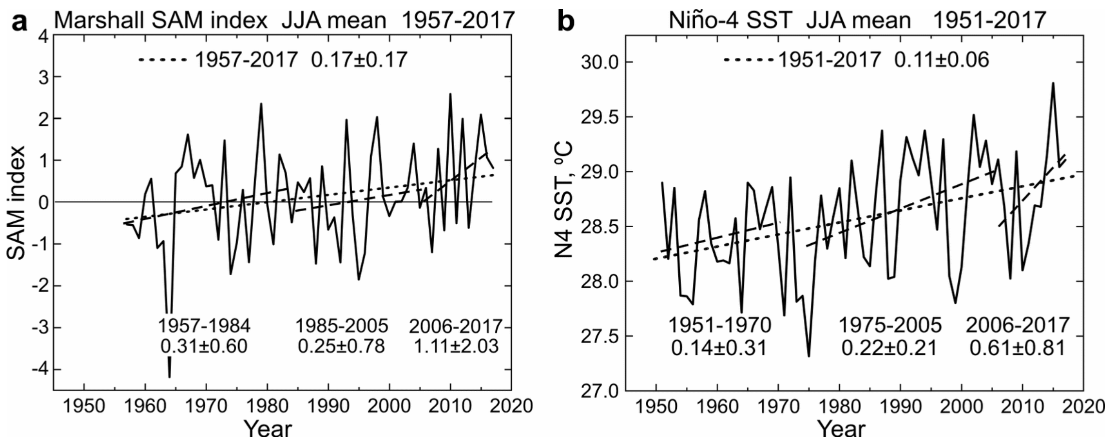

Fig. S3. Time series of seasonal mean climate indices for austral winter (JJA): **a.** SAM, 1957–2017, and **b.** N4, 1951–2017. Total (dotted lines) and piecewise (dashed lines) linear trends are indicated at the top and bottom of the plots, respectively.

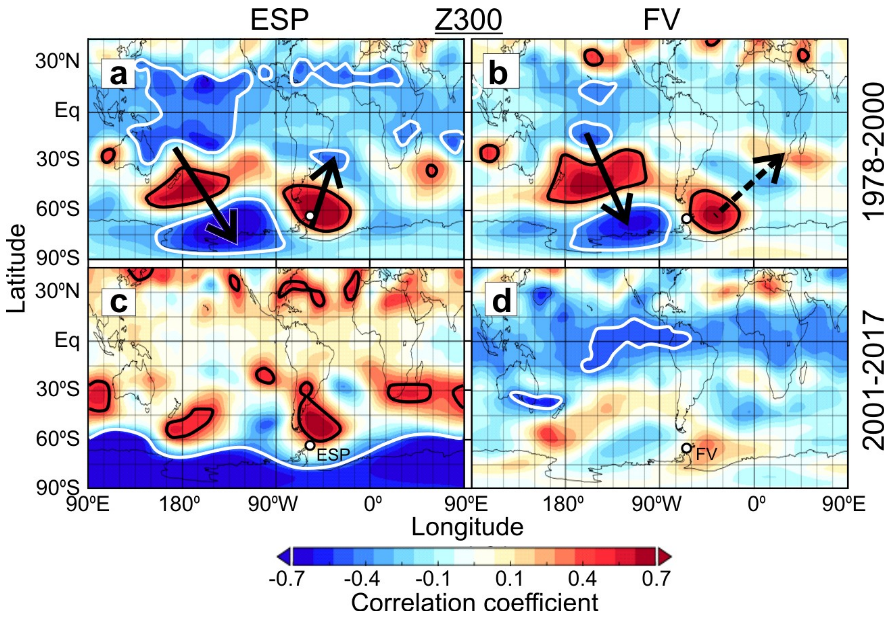

Fig. S4. Correlations between the temperatures at the AP station **a. & c.** Esperanza and **b. & d.** Faraday/Vernadsky and 300-hPa geopotential height (Z300) from the NCEP–NCAR reanalysis for periods of **a. & b.** 1978–2000 and **c. & d.** 2001–2017, when high and low correlations 'ESP vs FV', respectively, were observed (Fig. 4). Winter seasonal averages over June–August are presented. Positive (negative) correlation anomalies significant at the 95% confidence level are outlined by black (white) contours. Compare with the patterns of correlation with U300 in Fig. 6.

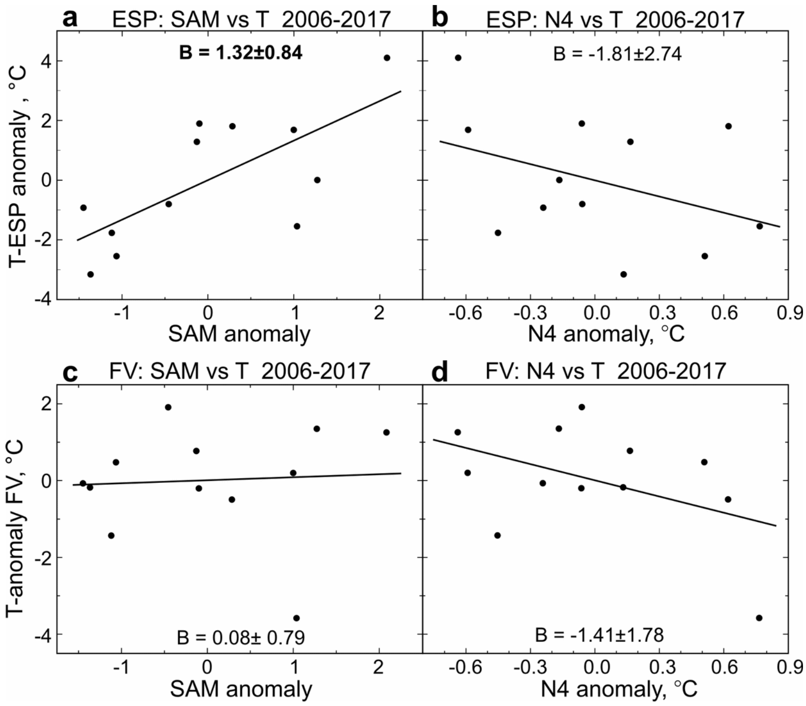

Fig. S5. Linear regression **a.** SAM vs ESP temperature**, b.** N4 vs ESP temperature, **c.** SAM vs FV temperature and **d.** N4 vs FV temperature for the period 2006–2017, when the NAP warming contrasts with the SAP cooling. Detrended time series are used.

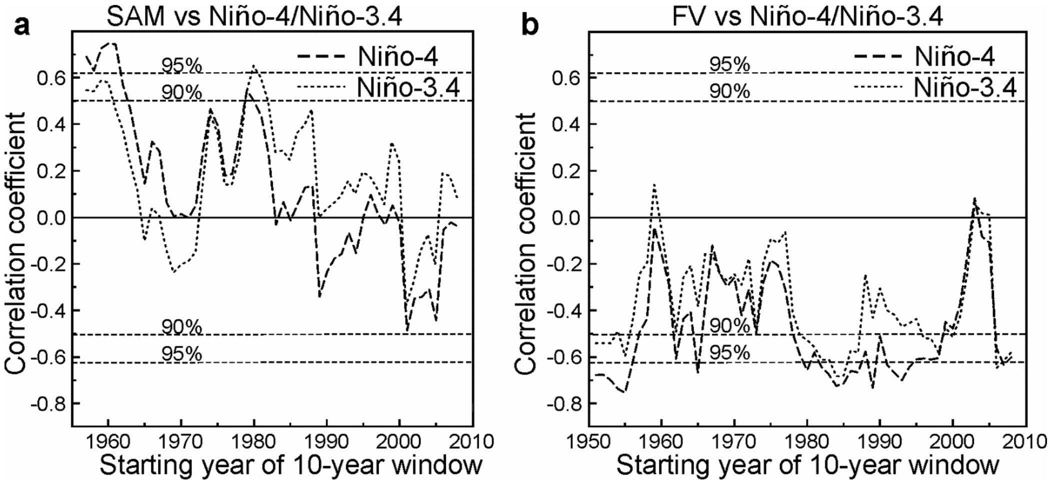

Fig. S6. Correlations with 10-year running window between **a.** SAM and N4/N3.4 indices and **b.** FV temperature and N4/N3.4 indices (dashed curve reproduces dashed curve in Fig. 8a) in winter (JJA).

Table S1. Linear trends of surface temperature at stations Esperanza and Faraday/Vernadsky from observations and from the NCEP–NCAR reanalysis (NNR) and ERA-Interim reanalysis in 2006–2017. The 95% confidence level is indicated.

	Observations	NNR	ERA-Interim
Esperanza	1.95±3.80	2.20±4.18	2.39±3.26
Faraday/Vernadsky	–1.46±2.54	–0.35±3.90	–0.17±1.06

Table S2. Detrended correlation coefficients *r* between the station temperatures and wind components from the reanalyses in 2006–2017. Zonal (U) and meridional (V) wind components at Esperanza and Faraday/Vernadsky are from NCEP–NCAR reanalysis (NNR, surface wind) and ERA-Interim reanalysis (ERA, 10-m wind). The reanalyses grid points are: 62.5°S, 57.5°W (NNR) and 63°S, 57°W (ERA) for Esperanza and 65°S, 65°W (NNR) and 65°S, 64°W (ERA) for Faraday/Vernadsky. The *r*-values significant at the 95% confidence level are in bold.

	T vs U-NNR	T vs U-ERA	T vs V-NNR	T vs V-ERA
Esperanza	**0.67**	**0.75**	–0.30	–0.51
Faraday/Vernadsky	–0.15	–0.19	**–0.76**	**–0.70**

Table S3. Linear trends in zonal (U) and meridional (V) wind components from the reanalyses. The wind components significantly correlated with the Esperanza and Faraday/Vernadsky temperatures in 2006–2017 (*r*-values shown in bold in Table S2) are presented. The 95% confidence level is indicated.

	U-component		V-component	
	NNR	ERA	NNR	ERA
Esperanza	0.96±4.0	1.56±3.38		
Faraday/Vernadsky			–0.51±1.85	–0.23±1.35